Cretaceous arachnid Chimerarachne yingi gen. et sp. nov. illuminates spider origins

Article *in* Nature Ecology & Evolution · April 2018

DOI: 10.1038/s41559-017-0449-3

CITATIONS
12

READS
897

7 authors, including:

Jason A Dunlop
Museum für Naturkunde - Leibniz Institute for Research on Evolution and Biodiver…
240 PUBLICATIONS **3,562** CITATIONS

SEE PROFILE

Paul A Selden
University of Kansas
202 PUBLICATIONS **3,392** CITATIONS

SEE PROFILE

William A. Shear
Hampden-Sydney College
111 PUBLICATIONS **1,029** CITATIONS

SEE PROFILE

nature ecology & evolution

ARTICLES

https://doi.org/10.1038/s41559-017-0449-3

Cretaceous arachnid *Chimerarachne yingi* gen. et sp. nov. illuminates spider origins

Bo Wang[1,2*], Jason A. Dunlop[3], Paul A. Selden[4,5], Russell J. Garwood[5,6], William A. Shear[7], Patrick Müller[8] and Xiaojie Lei[1,9]

Spiders (Araneae) are a hugely successful lineage with a long history. Details of their origins remain obscure, with little knowledge of their stem group and few insights into the sequence of character acquisition during spider evolution. Here, we describe *Chimerarachne yingi* gen. et sp. nov., a remarkable arachnid from the mid-Cretaceous (approximately 100 million years ago) Burmese amber of Myanmar, which documents a key transition stage in spider evolution. Like uraraneids, the two fossils available retain a segmented opisthosoma bearing a whip-like telson, but also preserve two traditional synapomorphies for Araneae: a male pedipalp modified for sperm transfer and well-defined spinnerets resembling those of modern mesothele spiders. This unique character combination resolves *C. yingi* within a clade including both Araneae and Uraraneida; however, its exact position relative to these orders is sensitive to different parameters of our phylogenetic analysis. Our new fossil most likely represents the earliest branch of the Araneae, and implies that there was a lineage of tailed spiders that presumably originated in the Palaeozoic and survived at least into the Cretaceous of Southeast Asia.

To date, 47,001 living and 1,342 extinct species of spider (Araneae) have been described (http://wsc.nmbe.ch/). The oldest fossils currently assigned to this group date from the late Carboniferous (approximately 305 million years ago (Ma))[1,2], while an earlier report of a Devonian (around 380 Ma) spider[3,4] was later reinterpreted as belonging to an extinct arachnid order named Uraraneida[5]. Uraraneids are also known from the Permian (approximately 275 Ma) and resemble spiders, but possess a long, flagellate telson. Another key difference is that uraraneids have spigots for producing silk[3], but lack the spinnerets that facilitate a more precise deposition of the threads[6,7]. Phylogenetic analysis[4,8] often recovers spiders as the sister group to a clade comprising whip spiders (Amblypygi), whip scorpions (Thelyphonida) and schizomids (Schizomida). Spiders and their relatives are known as the Pantetrapulmonata and are characterized by a ground pattern of two pairs of book lungs. Whip scorpions and schizomids express a flagelliform telson, a character also seen in the non-tetrapulmonate order Palpigradi, a group that has been postulated as retaining several plesiomorphic character states among arachnids[9]. Key autapomorphies of spiders, which presumably underlie their high modern species diversity, are silk glands opening via spigots on spinnerets, chelicerae with venom glands and male pedipalps modified for sperm transfer. Male spiders possess additional epiandrous silk spigots anterior to their genital opening. Spiders are conventionally divided into two suborders[6]. Mesothelae retain opisthosomal tergites and the spinnerets are in the middle of the ventral opisthosoma. Opisthothelae (Mygalomorphae and Araneomorphae) lack most external evidence of opisthosomal segmentation and the spinnerets emerge towards the posterior of the body. Recently, a handful of Palaeozoic fossils have been placed close to spider origins through preserving at least some of their diagnostic features. Uraraneida (Devonian–Permian) retained the presumably plesiomorphic flagelliform telson and possessed spigots, but no spinnerets[5]. Subsequent analyses[10,11] formally recovered Uraraneida and Araneae as a clade named Serikodiastida. Another spider-like fossil is *Idmonarachne brasieri* (Carboniferous)[12], which lacked both spinnerets and a telson. It was postulated as being more closely related to Araneae than the uraraneids, but also had divided opisthosomal tergites like members of the extinct arachnid order Trigonotarbida.

Results

Systematic palaeontology.

Arachnida Lamarck, 1801 (ref. [13])

Pantetrapulmonata Shultz, 2007 (ref. [8])

Chimerarachne yingi gen. et sp. nov.

Etymology. Genus: *Χίμαιρα* (chimera: a she-goat), in Greek mythology, a hybrid creature composed of the parts of more than one animal, and *ἀράχνη* (arachne: a spider), a weaver in Greek mythology; specific epithet, yingi, patronymic, honouring the collector, Yanling Ying.

Holotype. NIGP166870 (Fig. 1 and Supplementary Fig. 1). Deposited in the Nanjing Institute of Geology and Palaeontology, Chinese Academy of Sciences (NIGPAS).

Paratype. NIGP166871 (Fig. 2). Deposited in the NIGPAS.

Horizon and locality. Mid-Cretaceous (approximately 100 Ma); Burmese amber, from the Hukawng Valley, Kachin State, Myanmar.

Diagnosis. Arachnid with a segmented opisthosoma bearing two large, and one residual, pairs of spinnerets; opisthosoma terminating in a short pygidium bearing a long, annulated flagellum; pedipalp diverging distally into two bluntly rounded apophyses.

[1]State Key Laboratory of Palaeobiology and Stratigraphy, Nanjing Institute of Geology and Palaeontology, Chinese Academy of Sciences, Nanjing, China. [2]Key Laboratory of Zoological Systematics and Evolution, Institute of Zoology, Chinese Academy of Science, Beijing, China. [3]Museum für Naturkunde, Leibniz Institute for Research on Evolution and Biodiversity at the Humboldt University Berlin, Berlin, Germany. [4]Department of Geology, University of Kansas, Lawrence, KS, USA. [5]Earth Sciences Department, Natural History Museum, London, UK. [6]School of Earth and Environmental Sciences, University of Manchester, Manchester, UK. [7]Department of Biology, Hampden–Sydney College, Hampden–Sydney, VA, USA. [8]Friedhofstraße 9, Käshofen, Germany. [9]University of Sciences and Technology of China, Hefei, China. *e-mail: bowang@nigpas.ac.cn

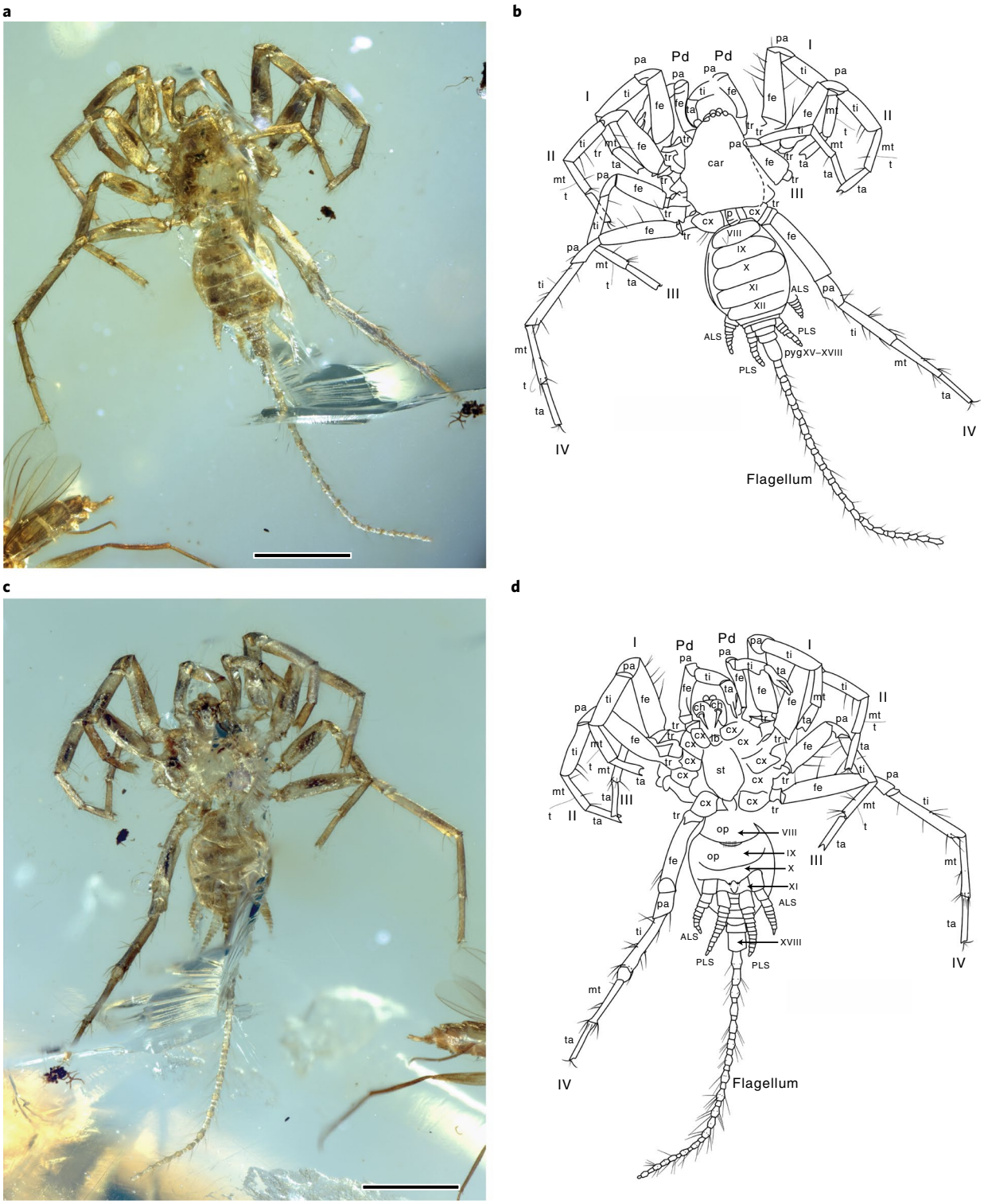

Fig. 1 | Holotype NIGP166870 of *C. yingi*. a,**c**, Entire specimen in dorsal (**a**) and ventral view (**c**). **b**,**d**, Respective interpretative drawings of the specimen shown in **a** and **c**. I–IV represent the leg numbers. ALS, anterior lateral spinneret; car, carapace; ch, chelicera; cx, coxa; fe, femur; lb, labium; mt, metatarsus; op, operculum; p, pedicel; pa, patella; Pd, pedipalp; PLS, posterior lateral spinneret; pyg, pygidium; st, sternum; t, trichobothrium; ta, tarsus; ti, tibia; tr, trochanter. Scale bars: 1 mm.

Description of the holotype. Adult male. Length (*L*) of body (including pygidium, but excluding flagellum): 2.42 mm. Cuticular ornament of fine scales. Carapace is widest posteriorly, narrowing to an acute anterior border of *L* 1.12 mm and width (*W*) 0.84 mm (*L*/*W* ratio: 1.28). Pair of median eyes close to the anterior margin, apparently also with two adjacent lateral eye tubercles, with an equivocal number of lenses.

Chelicerae of orthognath spider type, *L* 0.30 mm. Fang short, stout, gently curved and lacking setae. Chelicerae angled downwards at around 45° and thus largely concealed in the dorsal view.

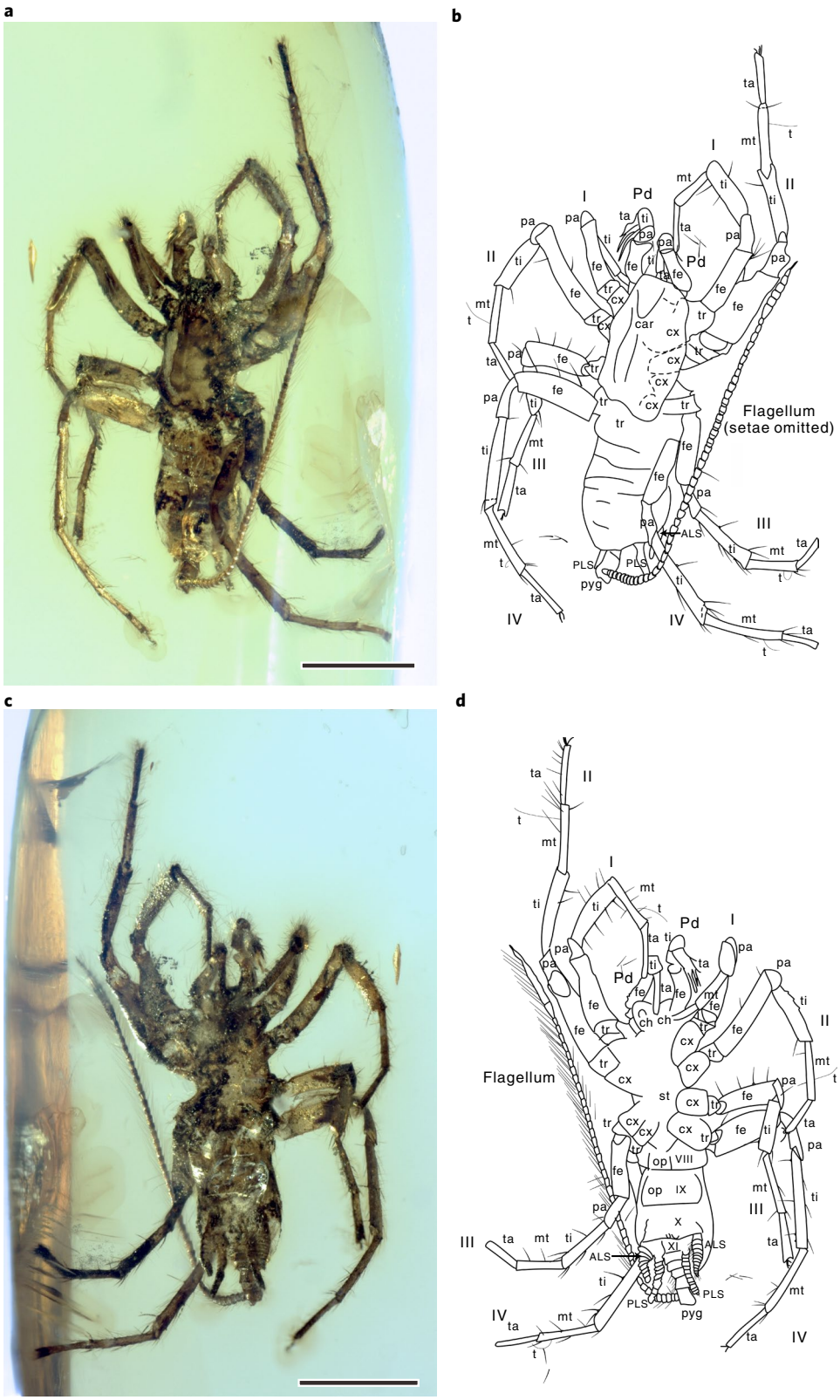

Fig. 2 | Paratype NIGP166871 of *C. yingi*. **a**,**c**, Entire specimen in dorsal (**a**) and ventral view (**c**). **b**,**d**, Respective interpretative drawings of the specimen shown in **a** and **c**. I–IV represent the leg numbers. ALS, anterior lateral spinneret; car, carapace; ch, chelicera; cx, coxa; fe, femur; lb, labium; mt, metatarsus; op, operculum; p, pedicel; pa, patella; Pd, pedipalp; PLS, posterior lateral spinneret; pyg, pygidium; st, sternum; t, trichobothrium; ta, tarsus; ti, tibia; tr, trochanter. Scale bars: 1 mm.

Pedipalps: femur *L*: 0.50 mm, patella *L*: 0.12 mm, tibia *L*: 0.36 mm, tarsus *L*: 0.40 mm (total *L* femur–tarsus: 1.41 mm). Pedipalp tibia with prolateral triangular flange, tarsus slightly inflated at about one-third of its length, distally bearing two blunt apophyses of

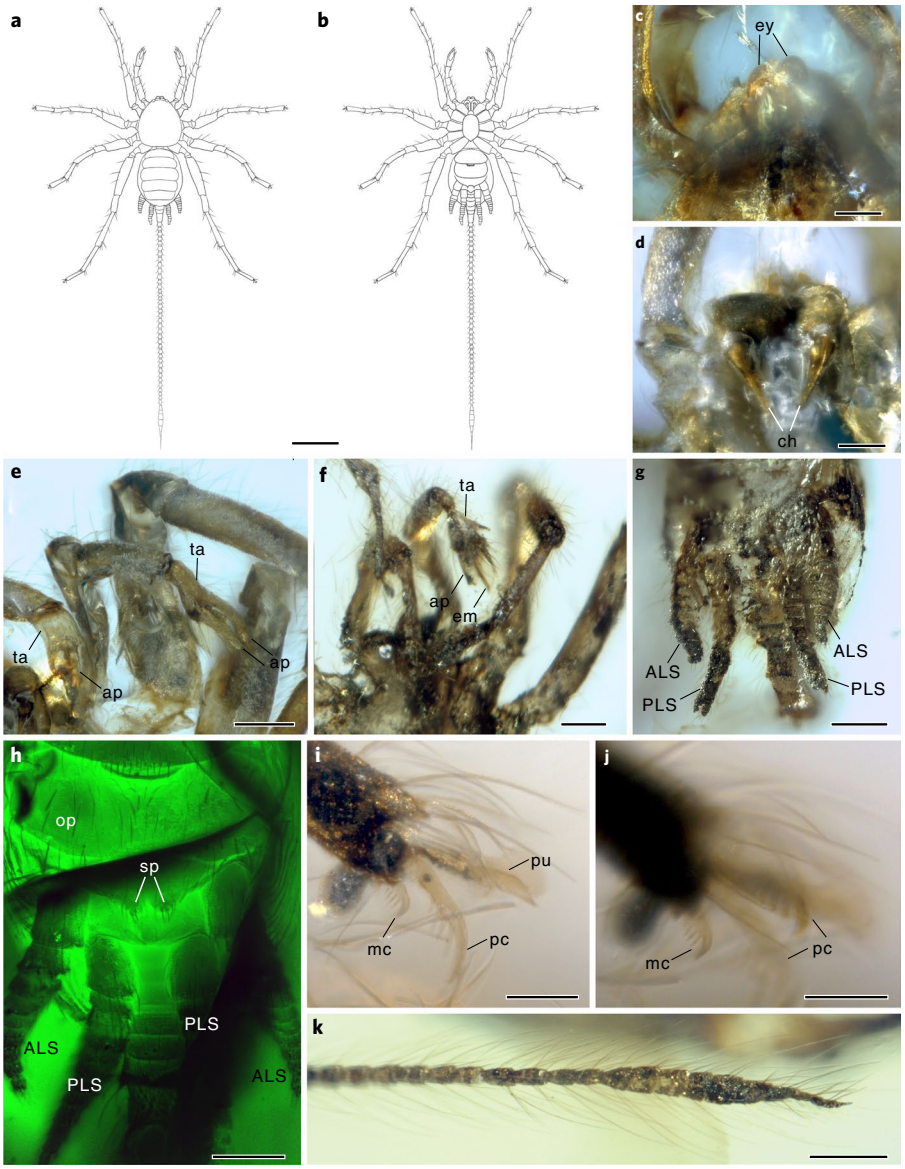

Fig. 3 | Morphological details and reconstruction. a,**b**, Reconstruction in dorsal (**a**) and ventral view (**b**). **c**, Eyes in NIGP166870. **d**, Chelicerae in NIGP166870. **e**, Ventral palps in NIGP166870. **f**, Ventral palps in NIGP166871. **g**, Spinnerets in NIGP166871. **h**, Confocal laser scanning microscope image of the abdomen in NIGP166870. **i**,**j**, Leg II claw in NIGP166870. **k**, Flagellum in NIGP166871. ap, apophysis; ALS, anterior lateral spinneret; ch, chelicera; em, embolus; ey, eye; mc, median claw; op, operculum; pc, paired claws; PLS, posterior lateral spinneret; pu, pulvillus; sp, spigots; ta, tarsus. Scale bars: 1 mm in **a** and **b**; 0.2 mm in **e**–**h** and **k;** 0.1 mm in **c** and **d**; 0.05 mm in **i** and **j**.

equal length (0.23 mm) and sausage-like shape (Figs. 3e,f and 4a). Legs pediform, leg formula IV II/I III, legs I and II subequal in length (2.42 mm and 2.43 mm, respectively). Legs bear gently curved bristles arising from small tubercles on all femur–tarsus, especially at the distal end of the metatarsus. Paired tarsal claws borne on onychium, claws gently curved, slender, hooked tip; small, gently curved median claw; both paired and median claws with four ventral spines increasing in length in distal half; also arising from the onychium, a spatulate lobe (pulvillus) as long as the paired claw (*L*: ~0.05 mm) (Figs. 3i,j and 4b,c). Trichobothrium present on all metatarsi at the 0.6 position. Cluster of at least five trichobothria at the distal end of at least tarsus II. Podomere lengths (tarsus excluding claw): leg I femur: 0.74 mm, patella: 0.28 mm, tibia: 0.60 mm, metatarsus: 0.45 mm, tarsus: 0.36 mm (total *L* femur–tarsus: 2.42 mm; metatarsus/tarsus ratio: 0.79); leg II femur: 0.78 mm, patella: 0.29 mm, tibia: 0.54 mm, metatarsus: 0.42 mm, tarsus: 0.40 mm (total *L* femur–tarsus: 2.43 mm; metatarsus/tarsus ratio: 0.95); leg III femur: 0.59 mm, patella: 0.28 mm, tibia: 0.54 mm, metatarsus: 0.45 mm, tarsus: 0.40 mm (total *L* femur–tarsus: 2.26 mm; metatarsus/tarsus ratio: 0.89); leg IV femur: 0.85 mm, patella: 0.34 mm, tibia: 0.78 mm, metatarsus: 0.62 mm, tarsus: 0.46 mm (total *L* femur–tarsus: 3.05 mm; metatarsus/tarsus ratio: 0.75). Mean metatarsus/tarsus ratio: 0.84.

Prosoma and opisthosoma connected by narrow pedicel (*L* 0.15 mm, *W* 0.13 mm). Opisthosoma suboval: *L* (including pygidium, but excluding flagellum) 1.22 mm, *W* 0.90 mm (*L*/*W* ratio: 1.36). Dorsal surface of opisthosoma bears seven visible tergites (segments VIII–XIV) with straight anterior and posterior borders and rounded lateral borders. Opisthosomal tergite measurements: 1: *L* 0.18 mm, *W* 0.53 mm; 2: *L* 0.20 mm, *W* 0.68 mm; 3: *L* 0.23 mm, *W* 0.78 mm, 4: *L* 0.20 mm, *W* 0.74 mm; 5: *L* 0.16 mm, *W* 0.64 mm; 6: *L* 0.04 mm, *W* 0.46 mm; 7: *L* 0.02 mm, *W* 0.40 mm. Posterior end of opisthosoma forms four-segmented pygidium with total *L* 0.43 mm; segment measurements: 1: *L* 0.06 mm, *W*

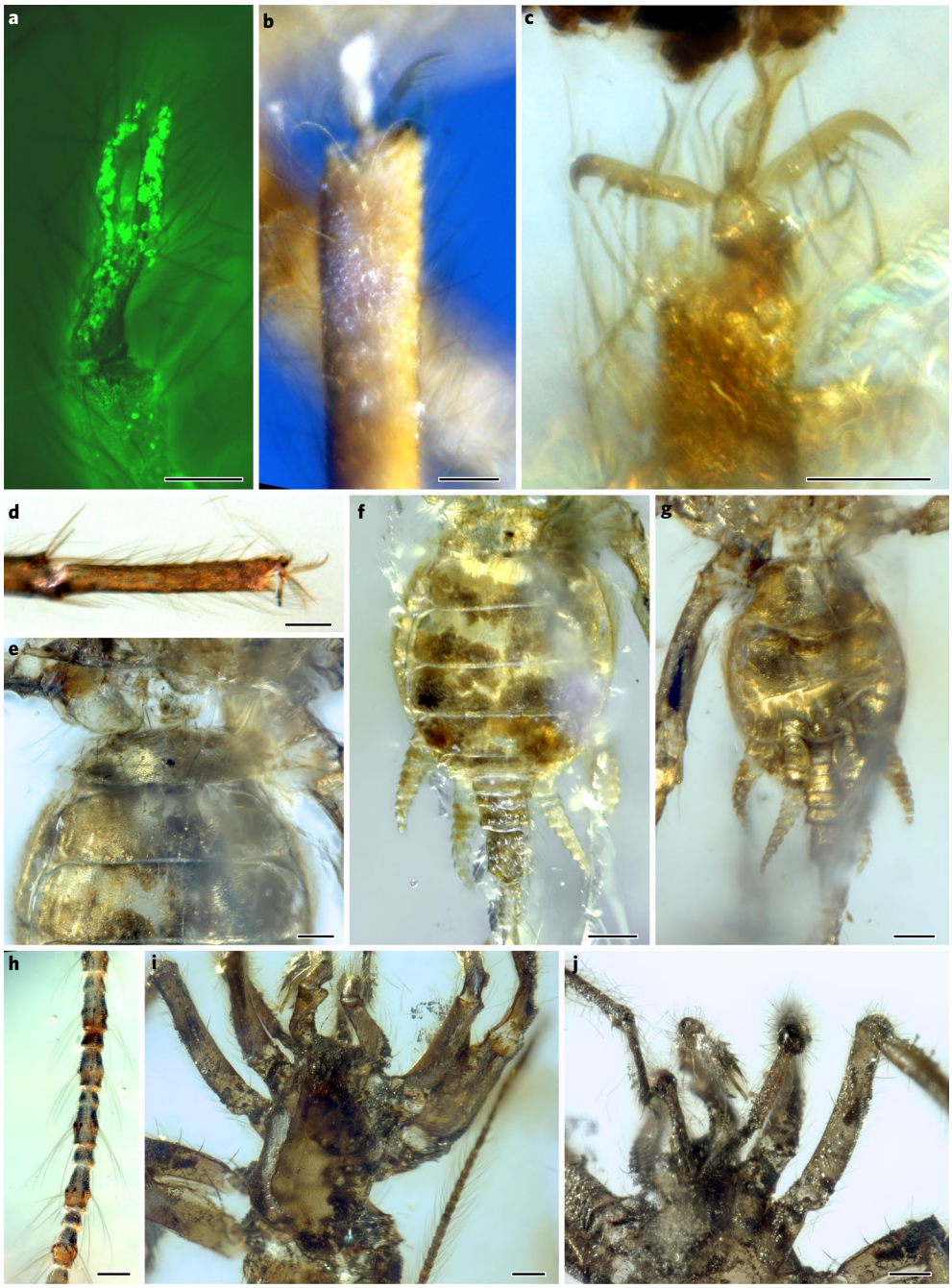

Fig. 4 | *C. yingi* NIGP166870 and NIGP166871. a–h, NIGP166870. **a**, Confocal laser scanning microscope of the cymbium. **b**, Leg II tarsus and claw. Note at least five trichobothria at the distal end of tarsus II. **c**, Right leg IV claw. **d**, Left leg IV claw. **e**, Dorsal pedicel. **f**, Dorsal abdomen. **g**, Ventral abdomen. **h**, Flagellum. **i**,**j**, NIGP166871. **i**, Dorsal prosoma. **j**, Dorsal palps. Scale bars: 0.2 mm in **f**, **g**, **i** and **j**; 0.1 mm in **a**, **d**, **e** and **h**; 0.05 mm in **b** and **c**.

0.25 mm; 2: *L* 0.06 mm, *W* 0.21 mm; 3: *L* 0.09 mm, *W* 0.20 mm; 4: *L* 0.21 mm, *W* 0.15 mm. Opisthosoma terminates in flagellum, *L* 2.86 mm, consisting of approximately 30 alternating short and long segments; long segments bear median bulge bearing ring of bristles (Fig. 1a).

Ventral opisthosoma bears 7 sternites (segments VIII–XIV, including opercula 1 and 2) preceding pygidium, measuring 1: *L* 0.35 mm, *W* 0.62 mm; 2: *L* 0.30 mm, *W* 0.74 mm; 3: *L* 0.16 mm, *W* 0.72 mm; 4: *L* 0.15 mm; 5: *L* 0.07 mm; 6: *L* 0.06 mm; 7: *L* 0.06 mm. Median posterior edge of first operculum bears oval structure, *W* 0.24 mm, covered by a row of around 10 bristles (Fig. 1c). Median posterior border of sternite 3 bears two pairs of spigots (equivalent to anterior median spinnerets). Median posterior border of sternite 4 bears a V-shaped, collulus-like structure (Fig. 3h). Anterior lateral spinnerets, *L* 0.65 mm, emerge from beneath the posterior edge of sternite 3, consisting of eight annular segments and a cone-shaped terminal segment. Posterior lateral spinnerets, *L* 0.70 mm, emerge from beneath the posterior edge of sternite 4, consisting of ten annular segments and a cone-shaped terminal segment.

Description of the paratype. Adult male. Body length (including pygidium, but excluding flagellum): 2.80. Cuticular ornament of fine scales. Carapace widest posteriorly (Fig. 4i), parallel-sided in posterior two-thirds, narrowing to acute anterior anteriorly: *L* 1.26 mm, *W* 0.74 mm (*L*/*W* ratio: 1.72). Subtriangular (apex rearward) ocular tubercle close to anterior margin. Eyes not clearly discernible.

Chelicera: *L* 0.27. Pedipalps: femur: *L* 0.39 mm, tarsus *L* 0.42 mm. Pedipalp tarsus distally bearing two blunt apophyses of subequal length, with median embolus of similar length between (Figs. 3f and 4j). Legs pediform, leg formula IV II I III. Legs bear gently curved bristles arising from small tubercles on all femur–tarsus, especially at the distal end of the metatarsus. Paired tarsal claws borne on onychium, claws gently curved, slender, hooked tip; small, gently curved median claw; both paired and median claws with four ventral spines increasing in length in distal half; also arising from onychium, a spatulate lobe (pulvillus) as long as the paired claw (*L* around 0.05 mm). Trichobothrium present on all metatarsi at the 0.6 position. Podomere lengths (tarsus excluding claw): leg I femur: 0.61 mm, patella: 0.34 mm, tibia: 0.58 mm, metatarsus: 0.45 mm, tarsus: 0.44 mm (total femur–tarsus: 2.45 mm; metatarsus/tarsus ratio: 0.98); leg II femur: 0.80 mm, patella: 0.29 mm, tibia: 0.69 mm, metatarsus: 0.57 mm, tarsus: 0.48 mm (total femur–tarsus: 2.84 mm; metatarsus/tarsus ratio: 0.84); leg III femur: 0.57 mm, patella: 0.29 mm, tibia: 0.55 mm, metatarsus: 0.46 mm, tarsus: 0.43 mm (total femur–tarsus: 2.30 mm; metatarsus/tarsus ratio: 0.93); leg IV femur: 0.64 mm, patella: 0.40 mm, tibia: 0.83 mm, metatarsus: 0.66 mm, tarsus: 0.48 mm (total femur–tarsus: 3.02 mm; metatarsus/tarsus ratio: 0.73). Mean metatarsus/tarsus ratio: 0.87.

Opisthosoma suboval, *L* (including pygidium, but excluding flagellum): 1.43 mm, *W* 0.72 mm (*L*/*W* ratio: 1.97). Posterior end of opisthosoma forms four-segmented pygidium of total *L* 0.34 mm. Opisthosoma terminates in flagellum, *L* 3.56 mm, of approximately 50 segments preceding a spindle-shaped terminal region consisting of 7 segments, terminal spine-like (Fig. 3k); highly setose throughout length. Ventral opisthosoma bears opercula 1 and 2 (segments VIII and IX). Median posterior border of sternite 3 bears two pairs of spigots (equivalent to anterior median spinnerets). Anterior lateral spinnerets, *L* 0.35 mm, emerge from beneath the posterior edge of sternite 3, consisting of annular segments and a cone-shaped terminal segment. Posterior lateral spinnerets, *L* 0.42 mm, emerge from beneath the posterior edge of sternite 4, consisting of annular segments and a cone-shaped terminal segment (Fig. 3g).

Remarks. Differences between the holotype and paratype can largely be attributed to taphonomy. Both are adult males and are presumed to belong to the same species. The paratype is more shrivelled (as is commonly seen in Burmese amber preservation). However, there is a distinct difference in the flagella of these two specimens: that of the holotype is shorter, lacks the terminal spindle-shaped thickening, has fewer segments (around 30 compared with around 60 in the paratype) and the segments are alternately short and long. We explain these differences by assuming that the flagellar segments were telescopic to some extent, so that the smaller segments can be hidden inside the distal end of the larger segments. Furthermore, the holotype must have lost the distal half of its flagellum. This would explain the missing terminal thickening and the fewer segments seen in this specimen. It is possible that *Chimerarachne* could lose its tail when threatened, as lizards do.

Discussion

C. yingi gen. et sp. nov. from mid-Cretaceous Burmese amber is a key fossil for understanding spider origins. It essentially resembles a spider with a tail (Supplementary Fig. 2). The 2.4–2.8 mm body is divided into a prosoma and opisthosoma connected by a narrow waist, or pedicel. The carapace is undivided and appears to show both median and lateral eye tubercles (Figs. 1b and 3c). The chelicerae are spider like and of the clasp-knife type (Fig. 3d). They lie in an orthognathous position, but point down at an angle of about 45°. The fang appears to be naked. The pedipalps are pediform, but end in a bifurcate tarsus (Figs. 3e,f and 4a), which we interpret as a cymbium covering a bulb and embolus. The legs are pediform, bearing several large macrosetae and trichobothria and end in toothed claws set on a projecting onychium, as well as a toothed median claw and empodium (Figs. 3i,j and 4c,d). The opisthosoma is segmented and terminates in a short, four-segmented post-abdomen bearing a flagellum (Figs. 3k and 4h), which is slightly longer than the body. Ventrally, the third opisthosomal segment bears a pair of prominent multi-articled spinnerets (Figs. 3g,h and 4g), which we interpret as equivalent to the anterior lateral spinnerets of spiders, plus a pair of less developed spigot-bearing mounds in a median position, which may be equivalent to the anterior median spinnerets. The fourth segment again has prominent spinnerets, equivalent to the posterior lateral spinnerets, but no corresponding median structures.

Retention of the telson is presumably plesiomorphic, thus a remarkable aspect of this discovery is that animals with such a body plan were still present in the terminal Mesozoic. *C. yingi* lived alongside Cretaceous spiders belonging to a number of modern families[14,15]. A corollary of this is that the new fossils are not ancestral to living spiders, which, as noted above, were present by the Carboniferous[1]. Rather, *C. yingi* presumably represents a survivor from an earlier (perhaps Palaeozoic) radiation of Pantetrapulmonata (Figs. 5 and 6).

The amber inclusions are also of considerable interest because they reveal key information about character acquisition on the spider stem and the likely ground pattern morphology of Araneae. The eyes in the fossil appear not to be on a single tubercle (Figs. 1b and 3c), as in mesothele spiders for example, consisting instead of a pair of median eyes and two lateral tubercles with an undetermined number of lenses. This condition is seen in whip spiders, whip scorpions and some spiders such as the mygalomorph superfamily Atypoidea and the araneomorph family Hypochilidae[16], both of which resolve as early branches in their respective parts of the spider tree of life[17].

The chelicerae of *C. yingi* are essentially spider like with a naked (hairless) fang (Fig. 3d), but the preservation does not reveal whether the fang had an opening for a venom gland. A key feature in the new fossils is the modification of the pedipalp into what we interpret here as a palpal organ with the tarsus forming a cymbium (Fig. 3e,f) plus the development of a bulb, presumably for transferring sperm. The deeply bifurcate nature of the tarsus/cymbium (Fig. 4a) in the new fossil is unique and potentially diagnostic for the genus (see above). However, we should note that in some mygalomorph spiders the tarsus is short and consists of two similar rounded lobes[18]. We note that the pedipalp of *C. yingi* is more like that of a mygalomorph spider than that of a mesothele[7]. This may have bearing on the question of whether the pyriform palpal bulb of mygalomorph spiders is closer to the plesiomorphic condition than the structurally more complex palp of mesotheles. For example, one study[19] inferred that the simpler bulbs of mygalomorphs contained secondarily fused elements. The present material is not preserved well enough to resolve this question, but future finds may prove to be informative here.

Perhaps the most interesting aspect of the new fossils is the position and configuration of the spinnerets (Figs. 3h and 4f,g). It has been suggested that the initial function of spider silk was not web building, but egg wrapping[20]. Mesothelae, as the sister group of all other spiders retaining plesiomorphic characters like segmentation, could support this scenario in having their spinnerets in the middle of the ventral opisthosoma[7] close to the genital opening. Spinnerets transposed posteriorly is a traditional synapomorphy of Opisthothelae. *C. yingi*, as a potential outgroup to all living spiders, challenges this scenario by preserving spinnerets in a more posterior (opisthothele) position. Another widespread assumption is that spiders originally had four pairs of spinnerets[21]: the anterior median and laterals and posterior median and laterals. In *C. yingi* both the anterior and posterior lateral spinnerets are well-developed and

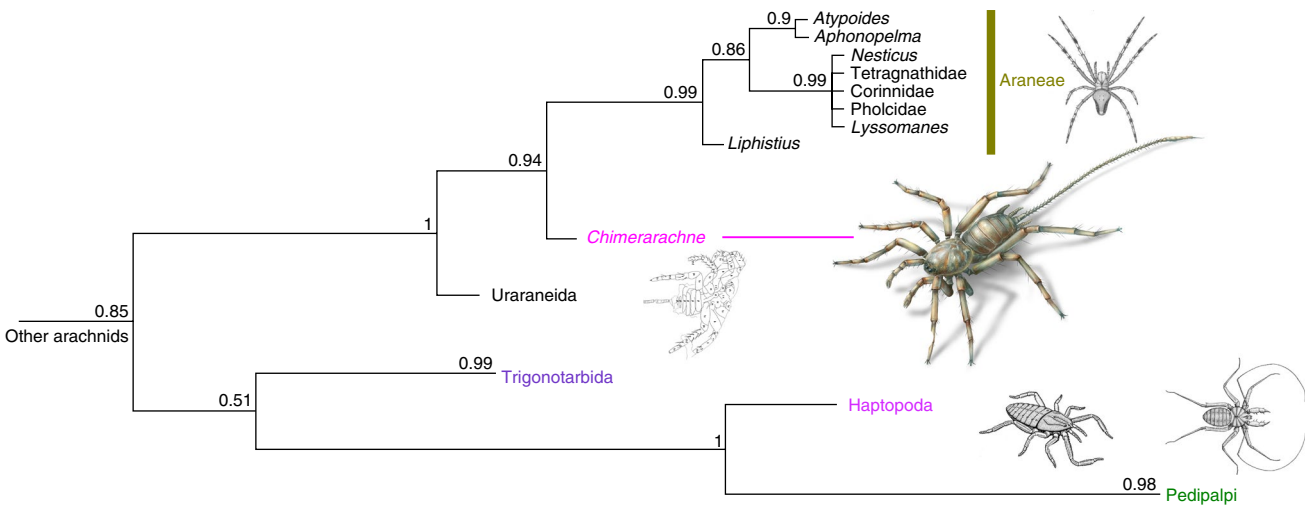

Fig. 5 | Phylogenetic relationships. Consensus cladogram (Bayesian majority rule consensus with support values) showing the position of *C. yingi* within the Pantetrapulmonata branch of the arachnids, which encompasses the spiders and their closest relatives (see Supplementary Fig. 3 for the full annotated tree). Both *Attercopus* and *Permarachne* are incomplete and scoring them individually collapses the tree, thus we combined characters from the two genera into one terminal Uraraneida. Full methods, results, discussion and sources for the line drawings are provided in the Supplementary Information.

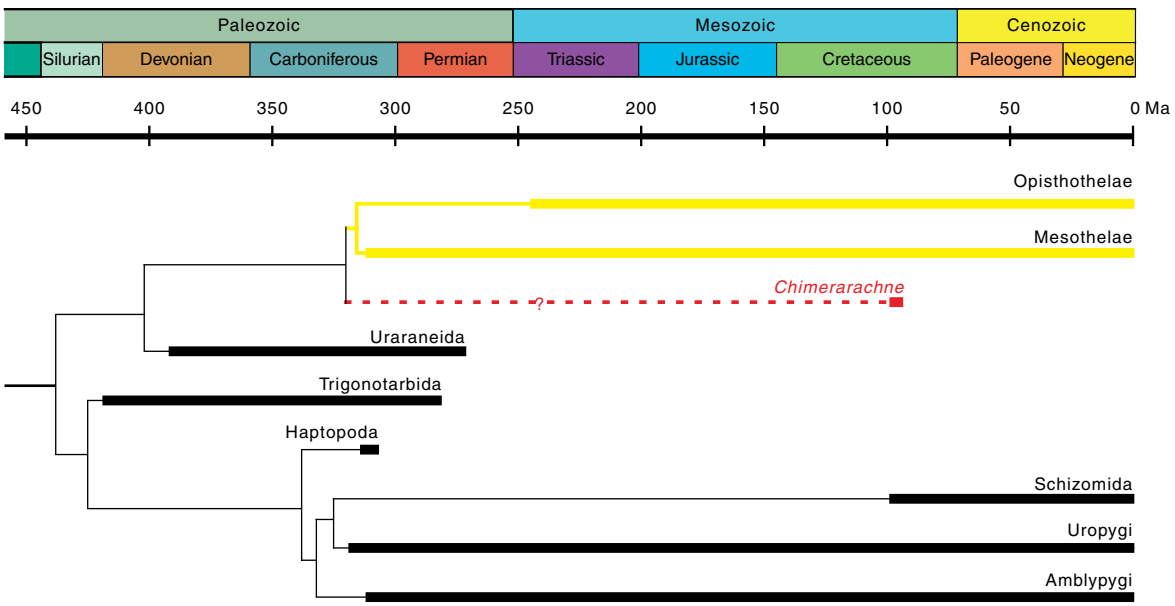

Fig. 6 | Evolutionary history of spiders and spider-related arachnids. Thick lines indicate the known extent of the fossil record. Branches representing modern spiders are yellow. The branch of *Chimerarachne* is red. See Supplementary Information for details of the phylogenetic analysis.

composed of multiple short articles (pseudosegments). They are similar to the spinnerets of modern mesotheles, but differ in having two or three large basal articles and in emerging from sclerotized ventral plates (Fig. 3h). In mesotheles there are only one or two large basal articles and no ventral sclerites associated with the spinnerets. Where we would expect anterior median spinnerets, there is only a pair of spigot-bearing mounds in the new fossil (Fig. 3h), while the posterior median spinnerets appear to be entirely absent.

A previous study[5] discussed a paradox in that spider spinnerets are modified opisthosomal appendages, probably representing the original telopod[22]. Outgroup comparison[23] implies that retaining these limbs should be plesiomorphic, but spider relatives such as uraraneids lack opisthosomal appendages. The authors postulated that there may be a genetic mechanism in spiders that reactivated the development of (lost) appendages, allowing the evolution of movable spinnerets that facilitate a more precise manipulation of silk strands. *C. yingi* preserves only part of the predicted ground pattern for spiders, leaving the question of whether the median spinnerets in the amber fossils are in the process of formation or reduction open. Loss of the ventral sclerites associated with the spinnerets on opisthosomal segments 3 and 4 clearly differentiates all modern spiders from the new fossils, and the retention of these sclerites in *Chimerarachne* may support the hypothesis that it reflects a plesiomorphic ventral anatomy.

Is *C. yingi* a spider? Phylogenetic reconstruction consistently recovers it in a clade with Uraraneida, Araneae and *Idmonarachne*, but different analysis techniques yield different internal topologies. Under parsimony with equal weights, the strict consensus tree resolves the new species as a sister group to the uraraneids, implied weights places it as a sister group of all extant spiders and the

alternative Bayesian majority rule consensus recovers Uraraneida, Araneae, *Idmonarachne* and *Chimerarachne* in a polytomy (see Supplementary Information for full results and discussion). This instability is likely to result from several key characters, such as the arrangement of the eyes and any modification of the male pedipalp, which are unknown in both uraraneids and *Idmonarache*. This problem is particularly acute in *Idmonarache*, where the preserved morphology is enigmatic[12]. To test the impact of this fossil, we excluded *Idmonarachne* from the analysis and recovered a uraraneid/spider/*Chimerarachne* polytomy under equal weights parsimony and *Chimerarachne* as an ingroup spider (specifically, a sister group to mesotheles) under implied weights. Our preferred tree (Fig. 5) is based on the Bayesian results (without *Idmonarachne*), which yield a phylogeny of the form (Uraraneida (*Chimarachne* (Mesothelae + Opisthothelae))) with strong support. We suggest that the collapse of this region of the tree when *Idmonarachne* is included probably reflects genuine uncertainty when all the terminal taxa are included, to which the Bayesian methodology may be more sensitive[24].

Conclusion

Irrespective of its exact relationships, we conclude that *Chimerarachne* reveals a grade of organization when spiders, or one of their closest relatives, developed a male palpal organ and at least part of the modern spinning apparatus, but retained the ancestral character of a whip-like telson. We reiterate that there must have been a continuum of character reduction and character acquisition on the lineage towards the modern spiders and we leave open the question of whether Araneae sensu stricto should be defined by loss of the telson or by the appearance of the spinnerets and/or male palpal organ.

Methods

Material studied. The two specimens (NIGP166870 and NIGP166871) are deposited in the NIGPAS. Both inclusions were obtained from an amber mine located near Noije Bum Village, Tanaing Town. The uranium–lead dating of zircons from the volcanoclastic matrix of the amber gave a maximum age of 98.8 ± 0.6 million years[25]. However, multiple lines of evidence, including the high degree of roundness of the amber and the presence of bivalve borings on the surface, suggest that the amber was most likely reworked before deposition in the volcanoclastic matrix, which implies that the age of the amber should be older than that of the matrix[26,27].

Observations. To reduce the deformation caused by differential refractivity, we sandwiched the amber specimens between two coverslips and filled the space with glycerol. Photographs were taken using a Zeiss SteREO Discovery.V16 microscope system at the State Key Laboratory of Palaeobiology and Stratigraphy, NIGPAS. In most instances, incident and transmitted light were used simultaneously. All images are digitally stacked photomicrographic composites of approximately 40 individual focal planes, which were obtained using the software Helicon Focus 6 (http://www.heliconsoft.com) for better illustration of the three-dimensional structures. Photomicrographs with a green background were taken using a Zeiss LSM 710 confocal laser scanning microscope with ×20 and ×10 objectives and a laser at 488 nm at the State Key Laboratory of Palaeobiology and Stratigraphy, NIGPAS.

To three-dimensionally reconstruct the fossil (Supplementary Video), we scanned the specimen NIGP166871 at the micro-computed tomography laboratory of NIGPAS using a Zeiss Xradia 520 Versa three-dimensional X-ray microscope. Unlike conventional micro-computed tomography, which relies on maximum geometric magnification and a flat panel detector to achieve high resolution, the three-dimensional X-ray microscope uses charge coupled device-based objectives to achieve higher spatial resolution. Depending on the size of the fossil specimen, a charge coupled device-based ×4 objective was used, providing isotropic voxel sizes of 3.7 µm with the help of geometric magnification. During the scan, the acceleration voltage for the X-ray source was 40 kV and a thin filter (LE1) was used to avoid beam hardening artefacts. To improve the signal-to-noise ratio, 2,500 projections of 3 s exposure over 360° were collected. Volume data processing was performed using the software VGStudio Max (version 3.0; Volume Graphics; https://www.volumegraphics.com).

Drawings and measurements were made from the photographs using Autodesk Graphic (www.graphic.com) on an Apple MacBook Pro computer. Due to the three-dimensional nature of amber-preserved specimens, appendage measurements are difficult to obtain because podomeres may lie at an angle to the viewer, so lengths of appendages must be considered as approximate.

Phylogenetic treatment. The new taxon was scored into an existing data matrix[11] modified to test the position of the Carboniferous fossil *Idmonarachne*[12] and the phylogeny of fossil whip spiders[28]. Full methods, results and discussion are provided in the Supplementary Information. In brief, four characters have been added to the matrix to test the placement of *Chimerarachne*. Trees were recovered using both parsimony (equal and implied weights) and Bayesian approaches, and interrogated through the exclusion of differing taxa and characters to explore their impact.

Life Sciences Reporting Summary. Further information on experimental design is available in the Life Sciences Reporting Summary.

Data availability. Taxonomic data have been deposited in ZooBank (http://zoobank.org) under the following Life Sciences Identifiers: urn:lsid:zoobank.org:pub:58DF4E2B-E284-486D-BD4E-FF2A2DBD8201 (article); urn:lsid:zoobank.org:act:8D6B77E2-C02F-48CD-BDB6-3590076F4E71 (genus); and urn:lsid:zoobank.org:act:9C0C78E5-6E05-4E92-BA34-456907C443E2 (species). The matrix is provided in both tnt and MrBayes formats (see Supplementary Data). Higher-resolution versions of the figures can be obtained upon request from the corresponding author.

Received: 7 September 2017; Accepted: 11 December 2017;

References

1. Selden, P. A. Fossil mesothele spiders. *Nature* **379**, 498–499 (1996).
2. Selden, P. A., Shcherbakov, D. E., Dunlop, J. A. & Eskov, K. Y. Arachnids from the Carboniferous of Russia and Ukraine, and the Permian of Kazakhstan. *Paläont. Z.* **88**, 297–307 (2014).
3. Shear, W. A., Palmer, J. M., Coddington, J. A. & Bonamo, P. M. A Devonian spinneret: early evidence of spiders and silk use. *Science* **246**, 479–481 (1989).
4. Selden, P. A., Shear, W. A. & Bonamo, P. M. A spider and other arachnids from the Devonian of New York, and reinterpretations of Devonian Araneae. *Palaeontology* **34**, 241–281 (1991).
5. Selden, P. A., Shear, W. A. & Sutton, M. D. Fossil evidence for the origin of spider spinnerets, and a proposed arachnid order. *Proc. Natl. Acad. Sci. USA* **105**, 20781–20785 (2008).
6. Platnick, N. I. & Gertsch, W. J. The suborders of spiders: a cladistics analysis. *Am. Mus. Novit.* **2607**, 1–15 (1976).
7. Haupt, J. The Mesothelae—a monograph of an exceptional group of spiders (Araneae: Mesothelae). *Zoologica* **154**, 1–102 (2003).
8. Shultz, J. W. A phylogenetic analysis of the arachnid orders based on morphological characters. *Zool. J. Linn. Soc.* **150**, 221–265 (2007).
9. Savory, T. On the arachnid order Palpigradi. *J. Arachnol.* **2**, 43–45 (1974).
10. Legg, D. A., Sutton, M. D. & Edgecombe, G. D. Arthropod fossil data increase congruence of morphological and molecular phylogenies. *Nat. Commun.* **4**, 2485 (2013).
11. Garwood, R. J. & Dunlop, J. A. Three-dimensional reconstruction and the phylogeny of extinct chelicerate orders. *PeerJ* **2**, e641 (2014).
12. Garwood, R. J. et al. Almost a spider: a 305-million-year-old fossil arachnid and spider origins. *Proc. R. Soc. B* **283**, 20160125 (2016).
13. Lamarck, J. B. *Système des Animaux sans Vertebres* (Deterville, Paris, 1801).
14. Wunderlich, J. New and rare fossil spiders (Araneae) in mid Cretaceous amber from Myanmar (Burma), including the description of new extinct families of the suborders Mesothelae and Opisthothelae as well as notes on the taxonomy, the evolution and the biogeography of the Mesothelae. *Beitr. Araneol.* **10**, 72–279 (2017).
15. Selden, P. A. & Ren, D. A review of Burmese amber arachnids. *J. Arachnol.* **45**, 324–343 (2017).
16. Miether, S. T. & Dunlop, J. A. Lateral eye evolution in the arachnids. *Arachnology* **17**, 103–119 (2016).
17. Wheeler, W. C. et al. The spider tree of life: phylogeny of Araneae based on target-gene analyses from an extensive taxon sampling. *Cladistics* **33**, 574–616 (2017).
18. Raven, R. J. The spider infraorder Mygalomorphae (Araneae): cladistics and systematics. *Bull. Am. Mus. Nat. Hist.* **182**, 1–180 (1985).
19. Kraus, O. *Liphistius* and the evolution of spider genitalia. *Symp. Zool. Soc. Lond.* **42**, 235–254 (1978).
20. Shultz, J. W. The origin of the spinning apparatus in spiders. *Biol. Rev.* **62**, 89–113 (1987).
21. Marples, B. J. The spinnerets and epiandrous glands of spiders. *J. Linn. Soc. Zool.* **46**, 209–222 (1967).
22. Sharma, P. P. Chelicerates and the conquest of land: a view of arachnid origins through an evo-devo spyglass. *Int. Comp. Biol.* **57**, 510–522 (2017).
23. Dunlop, J. A. & Lamsdell, J. C. Segmentation and tagmosis in Chelicerata. *Arth. Struct. Dev.* **46**, 395–418 (2017).
24. O'Reilly, J. E. et al. Bayesian methods outperform parsimony but at the expense of precision in the estimation of phylogeny from discrete morphological data. *Biol. Lett.* **12**, 20160081 (2016).

25. Shi, G. H. et al. Age constraint on Burmese amber based on U–Pb dating of zircons. *Cretac. Res.* **37**, 155–163 (2012).
26. Ross, A., Mellish, C., York, P. & Crighton, B. in *Biodiversity of Fossils in Amber from the Major World Deposits* (ed. Penney, D.) 208–235 (Siri Scientific Press, Manchester, 2010).
27. Wang, B. et al. Debris-carrying camouflage among diverse lineages of Cretaceous insects. *Sci. Adv.* **2**, e1501918 (2016).
28. Garwood, R. J., Dunlop, J. A., Knecht, B. J. & Hegna, T. A. The phylogeny of fossil whip spiders. *BMC Evol. Biol.* **17**, 105 (2017).

Acknowledgements

We are grateful to M. Engel and J. Wunderlich for helpful initial comments, Y. Huang and Y. Ying for providing specimens, Z. Yin and S. Wu for the micro-computed tomography reconstruction, J. Keating for advice on Bayesian inference of phylogeny and D. Yang for the reconstruction. This research was supported by the National Natural Science Foundation of China (41572010, 41622201 and 41688103), the Chinese Academy of Sciences (XDPB05) and the Youth Innovation Promotion Association of the Chinese Academy of Sciences (number 2011224).

Author contributions

B.W. designed the project. B.W., J.A.D., P.A.S., R.J.G. and W.A.S. all contributed to observation and interpretation of the fossils and drafted the manuscript. B.W. and X.L. produced the photographs. P.A.S. produced the line drawings, measurements and description. R.J.G. ran the phylogenetic analysis. P.M. collected data.

Competing interests

The authors declare no competing financial interests.

Additional information

Supplementary information is available for this paper at https://doi.org/10.1038/s41559-017-0449-3.

Reprints and permissions information is available at www.nature.com/reprints.

Correspondence and requests for materials should be addressed to B.W.

Publisher's note: Springer Nature remains neutral with regard to jurisdictional claims inpublished maps and institutional affiliations.